

PACS: 78.30.Na.81.05.Tp, 62.50.+p.

Micro-Raman study of CN_x composites subjected to high pressure treatment

N.I. Klyui¹, M.Ya. Valakh¹, V.G. Visotski¹, J. Pascual², N. Mestres³, N.V. Novikov⁴, I.A. Petrusha⁴, M.A. Voronkin⁴, N.I. Zaika⁴

¹ Institute of Semiconductor Physics, NAS Ukraine, 45 prospekt Nauki, 03028 Kyiv, Ukraine
Fax: 380(44) 265-83-42, E-mail: valakh@isp-div6.kiev.ua

² Departament de Física, Universitat Autònoma de Barcelona, 08193 Bellaterra, Spain

³ Institut de Ciència de Materials (CSIC), Campus UAB, 08193 Bellaterra, Spain.

⁴ Institute for Superhard Materials, NAS Ukraine, 2 Avtozavodskaya str., 254074 Kiev, Ukraine.

Abstract. CN_x films were deposited by reactive ion-plasma sputtering of a graphite target in an argon-nitrogen-acetone vapor atmosphere onto molybdenum substrates. After deposition the CN_x composites were cut from substrates, formed in pellets of 6 mm in diameter, and subjected to a high pressure-high temperature treatment at 7.7 GPa and 2000°C for 60 seconds. Micro-Raman spectroscopy, microhardness and X-ray diffraction were used for the sample characterization. After treatment the CN_x material leads to the formation of a number of highly ordered diamond crystals showing an extraordinarily low broadening of the 1332 cm^{-1} Raman-line ($\Delta\nu = 2.43 cm^{-1}$). Besides, the Raman spectra of the matrix surrounding the diamond crystals show an additional band at $\sim 1621 cm^{-1}$ with a Raman intensity that strongly depends on the distance from the crystals. We propose that this band is related to the formation of rhombohedral graphite in the treated sample and the corresponding effect of puckering of the graphite layers. The double-well potential model earlier proposed to describe diamond-like amorphous carbon has been used here for a qualitative description of the graphite-diamond phase-structural transformation.

Keywords: diamond growth and characterization, nitrogen-containing carbon, micro-Raman.

Paper received 30.11.99; revised manuscript received 10.12.99; accepted for publication 17.12.99.

1. Introduction

Considerable efforts have recently been focused on the synthesis and characterization of different CN_x materials. This interest has been mainly stimulated by attempts to obtain a hypothetical superhard $\beta-C_3N_4$ compound [1]. Notwithstanding the fact that up to date there are no clear evidences for obtaining this compound, a lot of promising results concerning the effects of nitrogen on amorphous carbon properties have been reported. It has been found that nitrogen substantially influences the optical properties of chemical vapor deposited carbon films, increasing the optical bandgap (up to 4 eV) [2] and determining the intriguing luminescent properties of a-C:H:N films [2,3]. A remarkable variation of the conductivity and an unusual decrease of disorder with nitrogen content were observed for a-C:H:N films [4]. The attempt to synthesize carbon nitride from nitrogen ion implantation has given rise to a drastic increasing of hardness in a-C:H implanted films [5, 6]. Finally, a decrease of the friction coefficient in nitrogen doped carbon films has also been measured, opening a potential interest in computer hard discs applications [7] as it was pro-

posed earlier for conventional carbon films [8].

As it was stated in the original work of Liu and Cohen [1], one of the possible ways to obtain carbon nitride crystal is to work under high pressure and high temperature conditions. In [9], shock wave compression of carbon nitride precursors was used to synthesize the $\beta-C_3N_4$ phase but these attempts were also unsuccessful. Probably, the failure to produce tetrahedral carbon nitride may be related to the formation of high diamond crystals concentration in shocked carbon nitride samples. These diamonds were well ordered as compared with diamonds synthesized from carbonaceous starting materials [9].

Taking into account the rather small size of the synthesized diamond crystals, experimental methods having high spatial resolution are needed to study such kind of samples. Among these methods micro-Raman spectroscopy is very promising due to its non-destructive character and its high sensitivity, especially to identify different carbon structural configurations.

In this work we present results of a micro-Raman study of highly ordered diamond crystals formed after high-pressure-high temperature treatment of CN_x precursors. Taking

the broadening of the 1332 cm⁻¹ Raman line as a measure of the degree of ordering, we show that the diamond crystals obtained in this work are better than the ones described in [9]. For a qualitative explanation of the phase structural transition from amorphous carbon to diamond crystals, we use the double-well potential model recently proposed by us to describe structural peculiarities of amorphous carbon [10]. For completeness, X-ray diffraction and microhardness measurements were also carried out.

2. Experiment

CN_x films were deposited by ion-plasma sputtering of a graphite target in an argon-nitrogen-acetone vapor atmosphere. A triode system of sputtering was used when the plasma discharge was excited by thermoelectric emission and localized as a plane beam using the magnetic field of a permanent magnet. Details of the film deposition have been described earlier [11]. The CN_x films were deposited onto molybdenum substrates heated up to 700°C by means of an electrical current. In order to avoid sputtering of the growing film, the low frequency bias voltage (20 kHz) did not exceed 50 V. The partial pressure of nitrogen in the chamber was 0.1 mTorr and the total gas pressure was 2.5 mTorr. The discharge power on the target was 1.2 kW. For high pressure experiments the CN_x composites were cut from substrates, pressed in a pellet of 6 mm in diameter and put into a special high-pressure apparatus described in details elsewhere [12]. In order to avoid the interaction of the sample with the apparatus chamber, the sample faces were protected using special graphite discs. The pellets were subjected to high temperature (2000°C) at a pressure of 7.7 GPa, for 60 seconds.

Raman scattering measurements were performed in backscattering configuration using a Jobin-Yvon T64000 spectrometer coupled with an Olympus metallographic microscope. The excitation was made using the 514.5 nm line of an Ar⁺ laser. The light was focused and collected by a 100-fold short focus objective with a numerical aperture of 0.90. The spot size on the sample surface for the objective used was of the order of 1 μm. The laser beam power on the samples was in the range 0.3-3.3 mW. The energy position, full width at half maximum (FWHM) and band intensity ratios were determined after deconvolution of the Raman spectra.

The microhardness of samples was measured using a Vickers' indenter and a Shimadzu HMV-2000 microhardness tester. The mean value of film hardness was determined by averaging the results of 10 tests. Standard X-ray diffraction data were collected using a DRON-3 system. All measurements were made at room temperature.

3. Results and discussion

Fig. 1 shows the Raman spectrum of initial deposited a-CN_x film (curve a), in the region of stretching C-C bands. The spectrum is standard for amorphous carbon and consists of two bands usually denoted as *G* («graphite») and *D* («dis-

ordered») [13]. The first one (*G*-band) is localized at $\nu \sim 1580$ cm⁻¹ and is associated to the E_{2g} in-plane graphite Raman active mode. The feature at ~ 1355 cm⁻¹ (*D*-band) is usually assigned to first-order scattering of zone-boundary phonons activated by the disorder induced by finite sp^2 crystallite size effects [13]. This band is observed due to selection rule violation and the relative intensity of the *D* band with respect to the *G* band correlates with sp^2 graphite clusters size in polycrystalline graphite [13]. However, a number of recent works testify that there are some problems using the I_D/I_G ratio as a quantitative criterion for sp^2 cluster size in amorphous a-C and a-C:H films [14, 15]. In this connection, it is appropriate to note that the double-well potential model describing the coexistence of sp^2 - and sp^3 - bonds in amorphous carbon [10] does not deal with nano-sized sp^2 -coordinated graphite clusters. Nevertheless, the spectrum of the initial film (see curve a in Fig. 1) shows a high I_D/I_G ratio (2.83) indicating high disorder in the film.

After the first stage of the measurement the films were cut from substrates and subjected to a high pressure treatment. Significant changes in the Raman spectrum of the processed sample were observed (see curve b in Fig. 1). In particular, the I_D/I_G ratio decreased dramatically down to 0.54. This change is the clear evidence of sample graphitization. This conclusion is directly supported by microhardness measurements, showing the decrease from 14.2 GPa for the initial film to 0.77 GPa for the treated sample. Besides, the intensity of the relevant «graphite» line in the X-ray diffraction pattern (not shown here) also increased after the high pressure treatment.

All these measurements were performed on the surface of the treated sample with no inclusions or structural features in it. At the opposite side of the sample numerous

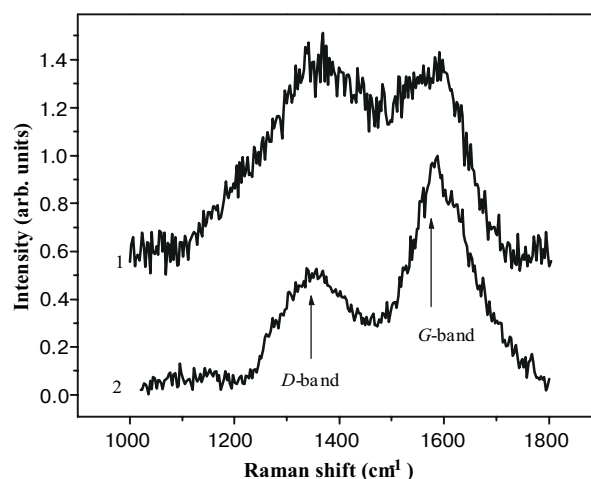


Fig. 1. Raman spectra of a-CN_x film after deposition (1) and the CN_x composite after high pressure-high temperature treatment (2). The spectrum 2 was measured from the pellet side opposite to the side where diamond crystals were observed. Parameters of the spectra: 1- $I_D/I_G = 2.83$; $\nu_G = 1590$ cm⁻¹; $\Delta\nu_G = 129$ cm⁻¹; $\nu_D = 1373$ cm⁻¹; $\Delta\nu_D = 281$ cm⁻¹; 2 - $I_D/I_G = 0.54$; $\nu_G = 1593$ cm⁻¹; $\Delta\nu_G = 153$ cm⁻¹; $\nu_D = 1356$ cm⁻¹; $\Delta\nu_D = 147$ cm⁻¹.

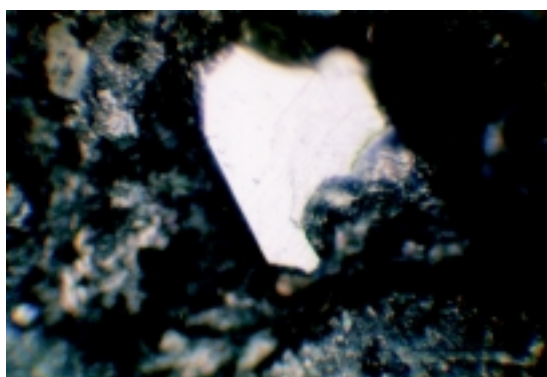


Fig. 2. Optical micrograph of the biggest diamond crystal.

diamond crystals were observed under the optical microscope or even by the naked eye. Among these crystals one stands out because of its relative large size ($\sim 400 \mu\text{m}$, see Fig. 2). It should be pointed out that most of the small diamond crystals were located in the immediate vicinity of the largest one. The Raman spectrum of the large crystal is presented in Fig. 3 (see curve a). For comparison, Raman spectra of diamond obtained by shock wave compression of different carbon precursors [9] are also shown (see curves b and c). Notice that our diamond crystal is extraordinarily well ordered relative to shock synthesized diamonds obtained in [9]. The broadening of the 1332 cm^{-1} Raman line for our crystal is very low ($\Delta\nu \sim 2,4 \text{ cm}^{-1}$) and close to the one observed for Ila diamond single crystal ($\Delta\nu \sim 2,7 \text{ cm}^{-1}$) [16]. An important feature of the Raman spectrum displayed in Fig.3a is the absence of Raman bands related to graphite or sp^2 bonded carbon. Taking into account the fact that Raman scattering is very sensitive to the graphitic carbon phase [16], we may conclude that there is no graphite or amorphous sp^2 bonded carbon neither on the surface nor in the synthesized crystal volume.

It should be emphasized that we do not observe diamond crystals in samples obtained from nitrogen free car-

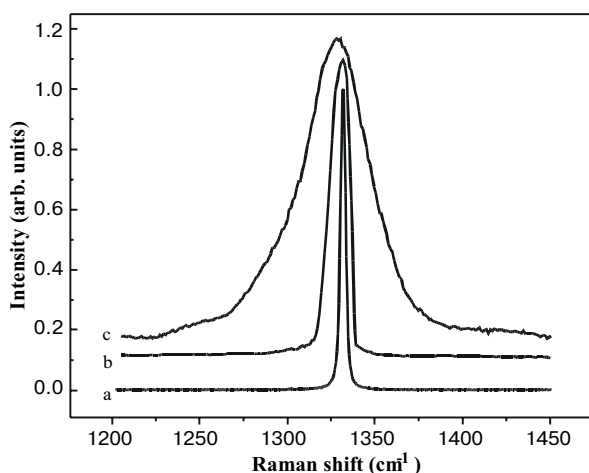


Fig. 3. a - Raman spectrum of the large diamond crystal shown in Fig.2. b, c - Spectra of diamond crystal obtained in [9] for shocked carbon nitride precursor (2) and graphite control sample (3).

bon precursors subjected to the same high pressure-high temperature treatment mentioned above. Thus, nitrogen stimulates diamond formation during the high pressure treatment. Taking into consideration the fact that there were no spectral peculiarities connected with carbon-nitrogen bonds in the Raman spectra of the processed sample, the nitrogen is most likely to escape from samples during treatment. It has been suggested that the aggregation of carbon into well-ordered diamond can be accompanied by a possible formation of molecular nitrogen [9]. On the one hand, this fact may compete unfavorably with the retention of nitrogen in the solid lattice [9]. On the other hand, the breaking of carbon-nitrogen bond, the formation of N_2 molecules and the nitrogen loss may induce the formation of highly active dangling carbon bonds. In its turn, these bonds can be preferentially reconstructed under high pressure into sp^3 -coordinated C-C bonds stimulating diamond phase formation.

Special attention was paid to Raman information on points in the region immediately adjacent to the large diamond crystal. Two series of spectra were analyzed. They were measured at a distance of 0.3 mm and 3 mm from the borders of the crystal shown in Fig. 2. The measurements were performed at the left, right, top, and bottom of the diamond crystal. Two representative spectra of the series are displayed in Fig. 4. We found that the Raman spectra measured near the large diamond crystal were radically modified as compared with the initial film spectrum (see curve a in Fig. 1). Remember that in most of matrix points, only some quantitative changes were observed in the Raman spectrum after high pressure treatment (see Fig. 1).

There are two main differences between the spectra displayed in Fig. 4 and spectrum b of Fig. 1. The first one is the dramatic narrowing of the G- and D-bands, and the second is the appearance of an additional band at 1621 cm^{-1} . The halfwidth of the corresponding bands are given in the cap-

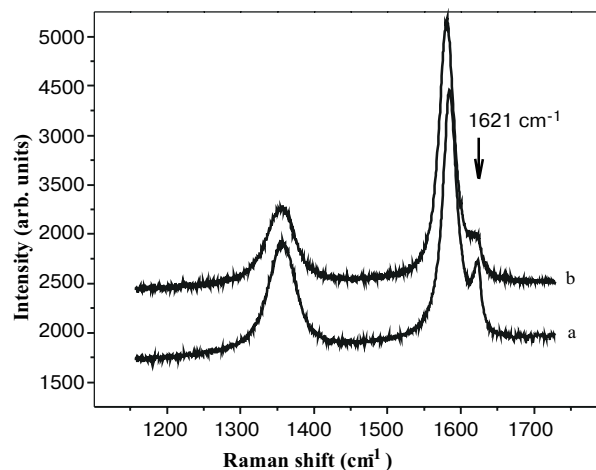


Fig. 4. Raman spectra measured in the vicinity of the large diamond crystal shown in Fig. 2. Distances from the crystal: a - 0.3 mm; b - 3 mm. Parameters of the spectra: a - $I_D/I_G = 0.83$; $I_{1621}/I_G = 0.131$; $\nu_G = 1584 \text{ cm}^{-1}$; $\Delta\nu_G = 23 \text{ cm}^{-1}$; $\nu_D = 1356 \text{ cm}^{-1}$; $\Delta\nu_D = 43 \text{ cm}^{-1}$; $\nu_{1621} = 1621 \text{ cm}^{-1}$; $\Delta\nu_{1621} = 12 \text{ cm}^{-1}$; b - $I_D/I_G = 0.59$; $I_{1621}/I_G = 0.063$; $\nu_G = 1581 \text{ cm}^{-1}$; $\Delta\nu_G = 25 \text{ cm}^{-1}$; $\nu_D = 1355 \text{ cm}^{-1}$; $\Delta\nu_D = 47 \text{ cm}^{-1}$; $\nu_{1621} = 1620 \text{ cm}^{-1}$; $\Delta\nu_{1621} = 15 \text{ cm}^{-1}$.

tion of the corresponding figures. Notice that the D and G bands presented in Fig. 4 are respectively 3 and 7 times narrower than the ones displayed in spectrum b of Fig. 1. Thus, if the later is characteristic of amorphous carbon with a sp^2 graphite cluster size much larger than that of the initial film (see curve a in Fig. 1), the spectra measured near the diamond crystal (see Fig. 4) are similar to the ones reported in polycrystalline graphite [17, 18].

Now we are going to discuss the results obtained on the basis of the theoretical model proposed by us in a previous work [10]. Let us start from prerequisites pointed out earlier concerning the graphite-diamond phase structural transformation [19]: 1) the transition from a sp^2 to a sp^3 coordinated phase is readily realized under a high pressure and high temperature treatments only if the initial material is graphite with a high degree of crystallinity; 2) the rhombohedral structural modification of graphite is the appropriate initial structure for a direct transformation along the stacking (c-axis) direction to form the diamond structure.

As it was mentioned above, the structure of the matrix is much closer to polycrystalline graphite than to amorphous carbon in the regions where diamond crystals have been formed (see Fig. 4). In our opinion, this is a direct confirmation of the first prerequisite. Let us consider the second prerequisite. In terms of the proposed double-well

potential model [10], the appearance of sp^3 coordination in graphite may be the result of the displacement of some carbon atoms in a direction perpendicular to the layer (parallel to the optic axis). Keeping it in mind we shall compare the structure of the hexagonal and rhombohedral modification of graphite [19]. In the hexagonal structure the layer stacking is ABAB, therefore, the atoms of the third layer occupy positions directly above the atoms of the first one. In the rhombohedral modification the layer stacking is ABCABC, that is the atoms of the third layer (C) occupy positions being symmetrically related to the first two layers (A and B). This distinction is illustrated by Fig. 5. From the point of view of possible atomic displacements perpendicular to the layer, the carbon atoms of hexagonal graphite can be separated into two groups. For one half of atoms the displacement magnitude must be very small because of the counteraction of atoms lying in adjacent layers. For the second half of atoms the displacement is relieved but is equiprobable for opposite directions. In terms of a dynamical approach [10], the mean equilibrium for the atomic position is within the layer. However, from this point of view there are fundamental differences between rhombohedral and hexagonal graphite. In rhombohedral graphite, the out-of-plane displacement is larger in one direction for one half of atoms; but for the other half it is just the opposite (see Fig. 5 where the

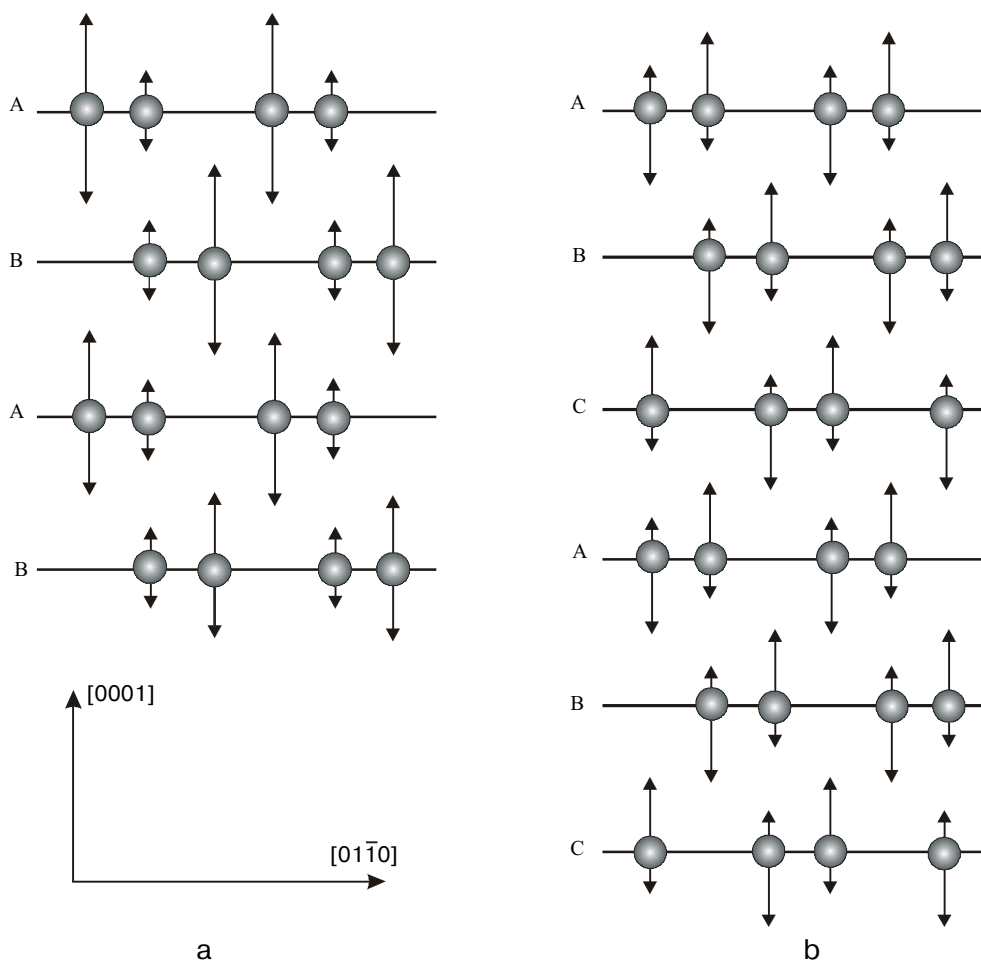


Fig. 5. Schematic plots of the probable out-of-plane atom displacement in hexagonal (a) and rhombohedral (b) graphite.

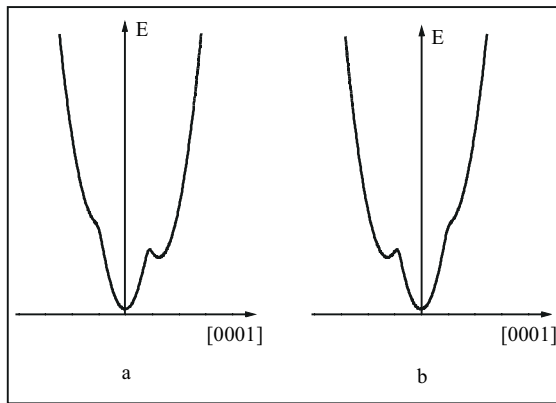


Fig. 6. Schematic diagram of the double-well potential function in real space for two adjacent carbon atoms in rhombohedral graphite lattice.

arrows show the displacement amplitudes of carbon atoms). In terms of our model [10], the situation for rhombohedral graphite can be illustrated in Fig. 6 where potential energy curves for carbon atoms are schematically presented. One can readily see from Figs 5 and 6 that the rhombohedral graphite structure is preferable for a direct transformation of plane sheets of hexagons into a puckered structure which is much closer to the structure of sp^3 -coordinated diamond [20]. Taking into account the conditions of high pressure-high temperature treatment, the mechanism discussed is probably responsible for the diamond nucleus formation. The diffusion mechanism can be involved in further growth (increase of the crystal size) of the diamond crystals, since the surrounding matrix is of low crystallinity [21].

Following, let us discuss the peculiarities of the spectra presented in Fig. 4 from the above-mentioned point of view. We assume that the origin of the *D* band in the Raman spectra presented in Fig. 4 differs from that discussed earlier for the corresponding *D* band in Fig. 1. For points localized near the diamond crystal, the *D* band may be stimulated by distortion of the sample structure instead of being directly associated to finite crystallite size effects. The distortion of the crystal structure was also invoked to explain the appearance of the *D* band in polycrystalline graphite as discussed in [18]. In our case such distortion may be connected both with the appearance of defect regions between adjacent hexagonal and rhombohedral graphite phases and with the effect of puckering of the graphite layers.

The same argument can also be used to explain the appearance of the new band localized at 1621 cm^{-1} in the spectra measured near the diamond crystal. This conclusion is supported by the experimental fact that there is a striking correlation between I_D/I_G and I_{1621}/I_G ratios. Indeed, as it is seen from Fig. 4 (see also the caption of Fig. 4) these values are substantially higher for probe points close to diamond crystals. It should be mentioned that this effect and the correlation between I_D/I_G and I_{1621}/I_G ratios were observed not only for the spectra presented in Fig. 4 but for all measured points as well. So, it seems reasonable to consider the Raman band at 1621 cm^{-1} band as a gauge for the formation

of the sp^3 coordination structure. In addition, it is interesting to note that within the same spectral range a new Raman line was observed in amorphous diamond obtained by high dose ion implantation of diamond crystals [22]. Moreover, the possible appearance of local vibrations associated to diamond structural defects was theoretically predicted [23] for the same spectral range.

Conclusions

During high pressure – high temperature treatment of amorphous nitrogen-containing carbon precursors the transformation of amorphous graphite-like structure to polycrystalline graphite and then to diamond takes place. The sharp *D* band and the additional band at $\sim 1621\text{ cm}^{-1}$ in the Raman spectra measured at matrix points surrounding the diamond crystals originate probably from the appearance of defect regions between adjacent hexagonal and rhombohedral graphite phases and the puckering effect of graphite layers. The double-well potential model earlier proposed for amorphous carbon consistently accounts for the observed peculiarities in diamond formation.

References

1. A.Y.Liu and M.L. Cohen, Structural properties and electronic structure of low compressibility materials: $\beta\text{-Si}_3\text{N}_4$ and hypothetical $\beta\text{-C}_3\text{N}_4$ // *Phys. Rev. B*, **41**(15), pp. 10727-10734 (1990).
2. N.I. Klyui, Yu. P. Piryatinskii and V.A. Semenovich, Intensive Visible Photoluminescence of a-C:H:N Films // *Materials Letters* **35** pp. 334-338 (1998).
3. F.Demichelis, Y.C. Liu, X.F. Rong, S. Scheiterand and A. Tragliafeiro, High energy photoluminescence in low Tauc gap a-C:H:N // *Sol. St. Comm.* **95** (7), pp. 475-477 (1995).
4. S.R.P.Silva, J.Robertson, G.A.J. Amaratunga, B.Rafferty, L.M.Brown, J.Schwan, D.F.Franceschini and G.Mariotto, Nitrogen modification of hydrogenated amorphous carbon films // *J.Appl.Phys.*, **81**(6), pp.2626-2634 (1997).
5. V.V. Artamonov, N.I. Klyui, V.P. Melnik, B.N. Romanyuk, M.Ya. Valakh, O. Vasilik, V.A. Semenovich, A. Perez-Rodriguez and J.R. Morante, Microraman and microhardness study of nitrogen implanted diamond-like carbon films // *Carbon* **36** (5-6), pp.791-794 (1998).
6. D.H. Lee, B. Park, D.B. Poker, L. Riester, Z.C. Feng and J.E.E. Baglin, Surface hardness enhancement in ion-implanted amorphous carbon // *J. Appl. Phys.* **80** (3), pp.1480-1484 (1996).
7. A. Khurshidov, K. Kato, S. Daisuke, Comparison of tribological properties of carbon and carbon nitride protective coatings over magnetic media // *J. Vac. Sci. Technol. A*, **14**(5), pp.2935-2939 (1996).
8. Hsiao-chu Tsai and D.B. Bogy, Characterization of diamond-like carbon films and their application as overcoats on thin-film media for magnetic recording // *J. Vac. Sci. Technol.* **A5** (6), pp. 3287-3312 (1987).
9. Michael R. Wixom, Chemical preparation and shock wave compression of carbon nitride precursors // *J. Am. Ceram. Soc.* **73** (7), pp.1973-1978 (1990).
10. A.Rakitin, M.Ya.Valakh, N.I.Klyui, V.G.Visotski, and A.P.Litvinchuk, Possibility of a double-well potential formation in diamondlike amorphous carbon // *Phys. Rev. B*, **58** (8), pp. 3526-3528 (1998).
11. N.V. Novikov, M.A. Voronkin, A.A. Smeknov, N.I. Zaika, A.P. Zakharchuk, Deposition by reactive ion-plasma sputtering and characterization of C-N films // *Diamond and Related Materials*, **4**, pp. 390-393 (1995).

12. G.S. Oleinik, I.A. Petrusha, N.V. Danilenko, A.V. Kotko, S.A. Shevchenko, Crystal-oriented mechanism of dynamic recrystallization nucleation in cubic boron nitride // *Diamond and Related Materials* **7**, pp.1684-1692 (1998).
13. F. Tuinstra and J.L. Koenig, Characterization of graphite fiber surfaces with Raman spectroscopy // *J. Compos. Mater.* **4**, P.492-498 (1970).
14. M.Yoshikawa, Raman spectra of diamondlike amorphous carbon films // *Mater. Sci. Forum* **v.52&53**, pp.365-386 (1989).
15. M.A. Tamor, J.A. Haire, C.H. Wu, K.C. Hass, Correlation of the optical gaps and Raman spectra of hydrogenated amorphous carbon films // *Appl. Phys. Lett.* **54** (2), pp. 123-125 (1989).
16. J.D. Hunn, S.P. Withrow, C.W. White and D.M. Hembree, Jr, Raman scattering from MeV-ion implanted diamond // *Phys.Rev.B* **52** (11), pp.8106-8111 (1995).
17. R.J. Nemanich, S.A. Solin, First and second-order Raman scattering from finite-size crystals of graphite // *Phys. Rev.B* **20** (2), pp.392-401 (1979).
18. Raphael Tsu, Jesus Gonzalez H., and Isaac Hernandez C, Observation of splitting of the E_{2g} mode and two-phonon spectrum in graphite // *Sol. St. Comm.* **27**, pp.507-510 (1978).
19. P.S. DeCarli and J.C. Jamieson, Formation of diamond by explosive shock // *Scienc.* **133** (3467), pp.1821-1823 (1961).
20. K. Lonsdale, H.J. Milledge and E. Nave, X-ray studies of synthetic diamond // *Miner. Mag.* **32** (1), pp.185-201 (1959).
21. A.V. Kurdyumov and A.N. Pilyankevich, *Phase transformation in carbon and boron nitride*, Naukova dumka, Kiev, 1979.
22. S.Prawer, K.W.Nugent and D.N.Jamieson, The Raman spectrum of amorphous diamond // *Diamond and Related Materials*, **7**, pp.106-110 (1998).
23. P. J. Lin-Chung, Local vibrational modes of impurities in diamond // *Phys. Rev.B* **50** (23) pp.16905-16913 (1994).